Interoffice

NATIONAL RADIO ASTRONOMY OBSERVATORY

TUCSON, ARIZONA

December 17, 1976

25 Meter Millimeter Wave Telescope
Memo #64

To: 25-M Working Group

From: B. L. Ulich

Subject: Review of atmospheric transmission at millimeter wavelengths

## I. INTRODUCTION

The Earth's atmosphere attenuates microwave radiation from cosmic sources. The magnitude of this attenuation varies with wavelength and with time according to global and local weather patterns. Since the efficiency of a radio telescope is directly proportional to atmospheric transmission, it is of great importance in selecting a suitable telescope site to understand the general characteristics of atmospheric attenuation and to thoroughly investigate the weather conditions at each site under consideration. Millimeter waves are severely scattered and absorbed by liquid water droplets in clouds and precipitation (Lo et al. 1975), and precise astronomical observations are generally impossible when optically opaque clouds are present. Since the dielectric constant of ice is much lower than that of liquid water, the millimeter-wave attenuation of cirrus ice clouds is negligibly small (Wulfsberg 1964 and Grody 1976) and precise astronomical observations can be made through ice clouds. In general, however, water clouds are so ruinous to Earth-based millimeter-wave astronomy that (in so far as atmospheric transmission is concerned) the primary site selection factor should be the relative time in which the sky is clear. Atmospheric attenuation in clear weather is due mainly to absorption by collision-broadened lines of terrestrial oxygen and water vapor (Straiton 1975). This report is a brief review of (selected) published theoretical calculations and measurements of clear-sky atmospheric absorption at millimeter wavelengths. The goal of this study was to reliably predict atmospheric transmission for proposed 25-M Telescope sites utilizing existing meteorological data.

## II. OXYGEN ABSORPTION

Oxygen and water vapor are exponentially distributed in the vertical direction in the terrestrial atmosphere with scale heights of about 5 km and 1.5-2.0 km, respectively (Kislyakov 1966). The total $O_2$ concentration and vertical distribution do not vary significantly with time. Thus the $O_2$ component of atmospheric absorption can be expressed as

$$\tau_o (\nu,h) = \alpha(\nu) \cdot \exp(-h/h_o) \qquad (1)$$

where $\tau_o$ = Atmospheric optical depth at zenith due to oxygen absorption (Nepers)

$\nu$ = Frequency (GHz)

$h$ = Site elevation (km)

$\alpha$ = Sea level atmospheric optical depth at zenith due to oxygen absorption (Nepers)

$h_o$ = Oxygen scale height (5 km).

The separability of the frequency - dependent term and the elevation - dependent term greatly facilitates accurate computation of $\tau_o$ for any telescope site. Rosenkranz (1975) has calculated the frequency - dependent parameter $\alpha$ ($\nu$) and his results are listed in Table I for seven different frequencies which span the expected operating range of the 25-M Telescope. All except two frequencies were chosen to match the natural "windows" between absorption lines where the terrestrial atmosphere is most transparent. The other two frequencies of interest are the 22.2 GHz transition of $H_2O$ (which is only weakly absorbing in the Earth's atmosphere but is masering in many celestial sources) and the 115.3 GHz J=1-0 line of CO which is useful for studying galactic and extragalactic structure. Note from Table I that $\alpha$(115.3 GHz) is large because of the close proximity to the strongly-absorbing 118.8 GHz $O_2$ line (Schulze and Tolbert 1963). When sensitive receivers are available at 230 GHz the J=2-1 transition of CO (which is intrinsically more intense than the J=1-0 line will offer the additional advantage of better atmospheric transparency at dry sites. Although many other authors have previously computed the oxygen spectrum (Meeks and Lilley 1963, Reber et al. 1970, Reber 1972), Rosenkranz's impact theory of overlapping spectral lines is the first completely theoretical calculation which matches the experimental observations both near the resonance lines and in their non-resonant wings. Measurements by Altshuler et al. (1968) at 35 GHz ($\alpha$ = 0.035) and by Shimabukuro and Epstein (1970) at 91 GHz ($\alpha$ = 0.037) are in good agreement with Rosenkranz's calculations. I would estimate the maximum error in $\alpha(\nu)$ to be less than 25% at all the frequencies listed in Table I. The uncertainty in the total atmospheric transmission due to the errors in $\alpha(\nu)$ is negligibly small.

## III. WATER VAPOR ABSORPTION

The expected atmospheric attenuation due to water vapor absorption has been calculated by many authors (Tolbert et al. 1964, Bastin 1966, Ulaby and Straiton 1970, Gaut and Reifenstein 1971, Emery 1972, and Waters 1976). There is generally good agreement with experimental data near resonance lines but discrepancies in the non-resonant wings can be as large as a factor of four. Gaut and Reifenstein (1971) have derived an empirical correction term which reduces the differences between the calculations and experimental data from 10 GHz to 1350 GHz to within about 10%. They state that the water vapor attenuation is a linear function of the precipitable water vapor in a vertical column. Thus the zenith optical depth due to water vapor absorption is given by

$$\tau_w (\nu, w) = \beta(\nu) \cdot w \tag{2}$$

where $\tau_w$ = Atmospheric optical depth at zenith due to water vapor absorption (Nepers)
$\nu$ = Frequency (GHz)
$w$ = Precipitable water vapor (mm)
$\beta$ = Atmospheric optical depth at zenith per millimeter precipitable water vapor (Nepers/mm)

The frequency - dependent term $\beta(\nu)$ from Gaut and Reifenstein (1971) is listed in Table I. Direct measurements utilizing radiosonde water vapor data by Shimabukuro and Epstein (1970) at 91 GHz ($\beta = 0.009$) and by Johnson et al. (1970) at 214 GHz ($\beta = 0.064$) are close to (but slightly lower than) the computed values. As can be seen in Table I, water vapor attenuation increases with frequency at short millimeter wavelengths and is the dominant source of opacity in the 2.00 mm, 1.30 mm, and 0.870 mm wavelength windows. Measurements of relative attenuation by Goldsmith et al. (1974) indicate that $\beta(345\,\text{GHz})/\beta(230\,\text{GHz}) = 2.2$ whereas the calculated value is 3.0. Mather et al. (1971) have compared the sky emission spectrum from 175 GHz to 428 GHz with theoretical calculations of water vapor absorption. Their data were averaged over long time periods and no simultaneous measurements of precipitable water vapor were made. Thus their results cannot be used to derive absolute values of $\beta(\nu)$, but their data are consistent with the shape of the frequency dependence and with the absolute values of $\beta(\nu)$ given in Table I. Wrixon (1974) measured the clear-sky zenith attenuation at 230 GHz on 9 days and correlated these data with measurements of the absolute surface humidity. He then assumed a linear vertical distribution of water vapor (rather than an exponential variation) to estimate the total precipitable water vapor. Reber and Swope (1972) have shown that estimates of total precipitable water from surface humidity measurements are not valid, and Goldsmith et al. (1974) and Fogarty (1975) have shown that surface humidity is a poor indicator of atmospheric attenuation. Thus Wrixon's value of $\beta(230\,\text{GHz}) = 0.022$ Nepers/mm is not a reliable predictor of 1.3 mm atmospheric attenuation. In addition, his value of $\alpha(230\,\text{GHz}) = 0.08$ is much higher than any theoretical calculation for oxygen absorption. In summary, the reliable experimental measurements of water vapor attenuation are in reasonably good agreement with the values of $\beta(\nu)$ in Table I (which I estimate to be accurate within about 25%). If systematic errors do exist in the computations, the experimental data tend to indicate actual attenuations less than the theoretical predictions in Table I.

## IV. CALCULATION OF ATMOSPHERIC TRANSMISSION

The total zenith optical depth due to oxygen and water vapor absorptions is simply the sum of Equations (1) and (2)

$$\tau (\nu, h, w) = \alpha(\nu) \cdot \exp(-h/h_o) + \beta(\nu) \cdot w \tag{3}$$

where

$\tau$ = Total atmospheric optical depth at zenith (Nepers)
$\nu$ = Frequency (GHz)
$h$ = Site elevation (km)
$w$ = Precipitable water vapor (mm)
$\alpha$ = Sea level optical depth at zenith due to oxygen absorption (Nepers)
$h_o$ = Oxygen scale height (5 km)
$\beta$ = Optical depth at zenith per millimeter precipitable water (Nepers/mm).

The normalized atmospheric transmissivity $\Gamma$ at a zenith angle Z is

$$\Gamma = \exp\left[-\tau\ (\nu,\ h,\ w) \cdot \sec\ (Z)\right] \tag{4}$$

where $\Gamma$ = Atmospheric transmissivity
$\tau$ = Total atmospheric optical depth at zenith
$Z$ = Zenith angle ($^{\circ}$).

Thus by specifying $\nu$, h, and w for a particular site, the transmission factor $\Gamma$ can be calculated from Equations (3) and (4) using the values of $\alpha$ and $\beta$ from Table I.

## V. COMPARISON OF MAUNA KEA AND KITT PEAK

At the present time at least two mountains must be given serious consideration as locations of the 25-M Telescope. They are Mauna Kea, Hawaii and Kitt Peak, Arizona. Relevant meteorological data from the NSF 25-M Telescope proposal are given in Table II. The water vapor concentrations are not grossly different at the two sites because the higher elevation of Mauna Kea is largely offset by the higher humidity of tropical air. The principal advantage of Mauna Kea is its lower latitude; a larger section of the sky is visible and most sources of interest will be observable for longer times and will transit at higher elevations. Figures 1-7 are plots of atmospheric transmissivity $\Gamma$ at source transit versus source declination for both sites at each of the seven standard frequencies. For all except the most southerly sources the atmospheric transmissivity at Mauna Kea is only slightly better than at Kitt Peak. Of course, time is what counts for most experiments and thus a better indicator of site performance would be $(\Gamma)^2$ rather than $\Gamma$. Figure 8 is a plot of the ratio of $(\Gamma)^2$ at Mauna Kea to $(\Gamma)^2$ at Kitt Peak versus frequency for a source at $\delta = 0^{\circ}$ at transit. Over the design range of the 25-M Telescope (up to 250 GHz) the increased efficiency at Mauna Kea is not substantial. Only at 345 GHz (where the telesope performance will be less than ideal) does Mauna Kea provide a significant improvement in average atmospheric transparency over that at Kitt Peak. In my opinion the possibly significant advantage of Mauna Kea is increased sky coverage rather than substantially better atmospheric transparency.

# REFERENCES


Altshuler, E. E., Falcone, V. J., Jr., and Wulfsberg, K. N. (1968). IEEE Spectrum, 5, 83-90.

Bastin, J. A. (1966). Infrared Phys., 6, 209-221.

Emery, R. (1972). Infrared Phys., 12, 65-79.

Fogarty, W. G. (1975). IEEE Trans. Antennas Propagat., AP-23, 441-444.

Gaut, N. E. and Reifenstein, E. C. (1971). NASA Contractor Report CR-61348, Environmental Research and Technology, Inc., Waltham, Mass.

Goldsmith, P. F., Plambeck, R. L.,and Chiao, R. Y. (1974). IEEE Trans. Microwave Theory Tech., 22, 1115-1116.

Grody, N. C. (1976). IEEE Trans. Antennas Propagat., AP-24, 155-162.

Johnson, W. A., Tsutomu, T. M., and Shimabukuro, F. I. (1970). IEEE Trans. Antennas Propagat., AP-18, 512-514.

Kislyakov, A. G. (1966). Izvestiya VUZ Radiofizika, 9, 451-461.

Lo, L., Fannin, B. M., and Straiton, A. W. (1975). IEEE Trans. Antennas Propagat., AP-23, 782-786.

Mather, J. C., Werner, M. W., and Richards, P. L. (1971). Ap. J. (Letters), 170, L59-L65.

Meeks, M. L. and Lilley, A. E. (1963). J. Geophys. Res., 68, 1683-1703.

Reber, E. E., Mitchell, R. L., and Carter, C. J. (1970). IEEE Trans. Antennas Propagat., AP-18, 472-478.

Reber, E. E. (1972). J. Geophys. Res., 77, 3831-3845.

Reber, E. E. and Swope, J. R. (1972). J. Appl. Meteor., 11, 1322-1325.

Rosenkranz, P. W. (1975). IEEE Trans. Antennas Propagat., AP-23, 498-506.

Schulze, A. E. and Tolbert, C. W. (1963). Nature, 200, 747-750.

Shimabukuro, F. I. and Epstein, E. E. (1970). IEEE Trans. Antennas Propagat., AP-18, 485-490.

Straiton, A. W. (1975). IEEE Trans. Antennas Propagat., AP-23, 595-597.

Tolbert, C. W., Krause, L. C., and Straiton, A. W. (1964). J. Geophys. Res., 69, 1349-1357.

Ulaby, F. T. and Straiton, A. W. (1970). IEEE Trans. Antennas Propagat., AP-18, 479-485.

Waters, J. W. (1976). "Methods of Experimental Physics: Part B: Radio Telescopes," edited by M. L. Meeks, Academic Press, New York, 142-176.

Wrixon, G. T. (1974). Paper presented at Fourth European Microwave Conference, Montreux, Switzerland, Sept. 1974.

Wulfsberg, K. N. (1964). Proc. IEEE, 52, 321-322.

TABLE I

ATMOSPHERIC TRANSMISSION DATA

| | | | | | | | |
|---|---|---|---|---|---|---|---|
| $\nu$ (GHz) | 22.2 | 31.4 | 90.0 | 115.3 | 150 | 230 | 345 |
| $\lambda$ (mm) | 13.5 | 9.55 | 3.33 | 2.60 | 2.00 | 1.30 | 0.870 |
| $\alpha$ (Nepers) | 0.013 | 0.028 | 0.041 | 0.345 | 0.008 | 0 | 0 |
| $\beta$ (Nepers/mm) | 0.0060 | 0.0015 | 0.012 | 0.019 | 0.033 | 0.067 | 0.20 |

TABLE II

25-M TELESCOPE SITE DATA

| Site | Latitude | Elevation (m) | Number of clear days[1] | $\langle w \rangle$[2] (mm) |
|---|---|---|---|---|
| Mauna Kea | $19^{\circ}$ 49' N | 4154 | 230 | 2.5±0.2 |
| Kitt Peak | $31^{\circ}$ 58' N | 2057 | 260 | 3.3±0.8 |

[1] Cloud cover less than 30%.

[2] Median daytime value for non-summer months.

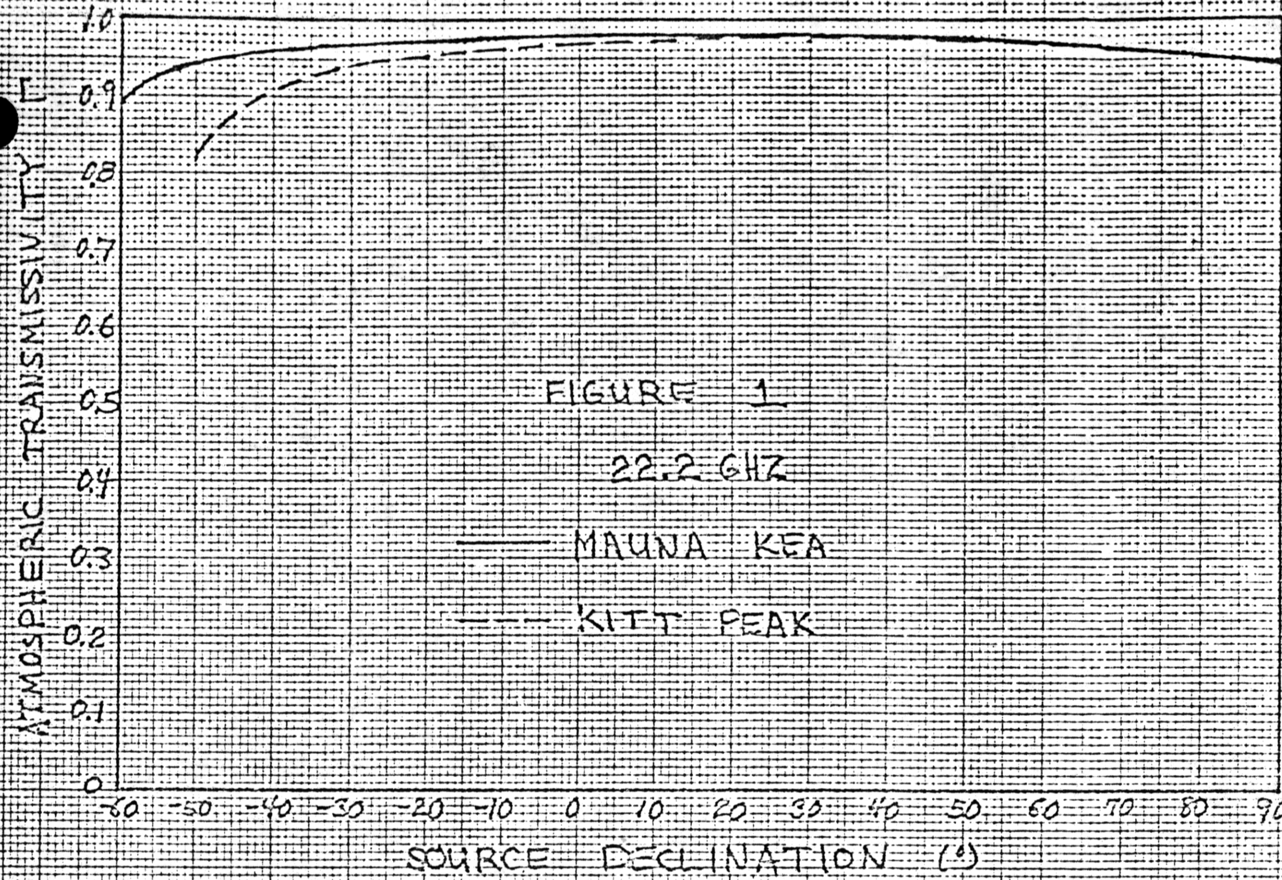
FIGURE 1
22.2 GHZ
MAUNA KEA
KITT PEAK
ATMOSPHERIC TRANSMISSIVITY Γ
1.0
0.9
0.8
0.7
0.6
0.5
0.4
0.3
0.2
0.1
0
-60 -50 -40 -30 -20 -10 0 10 20 30 40 50 60 70 80 90
SOURCE DECLINATION (°)

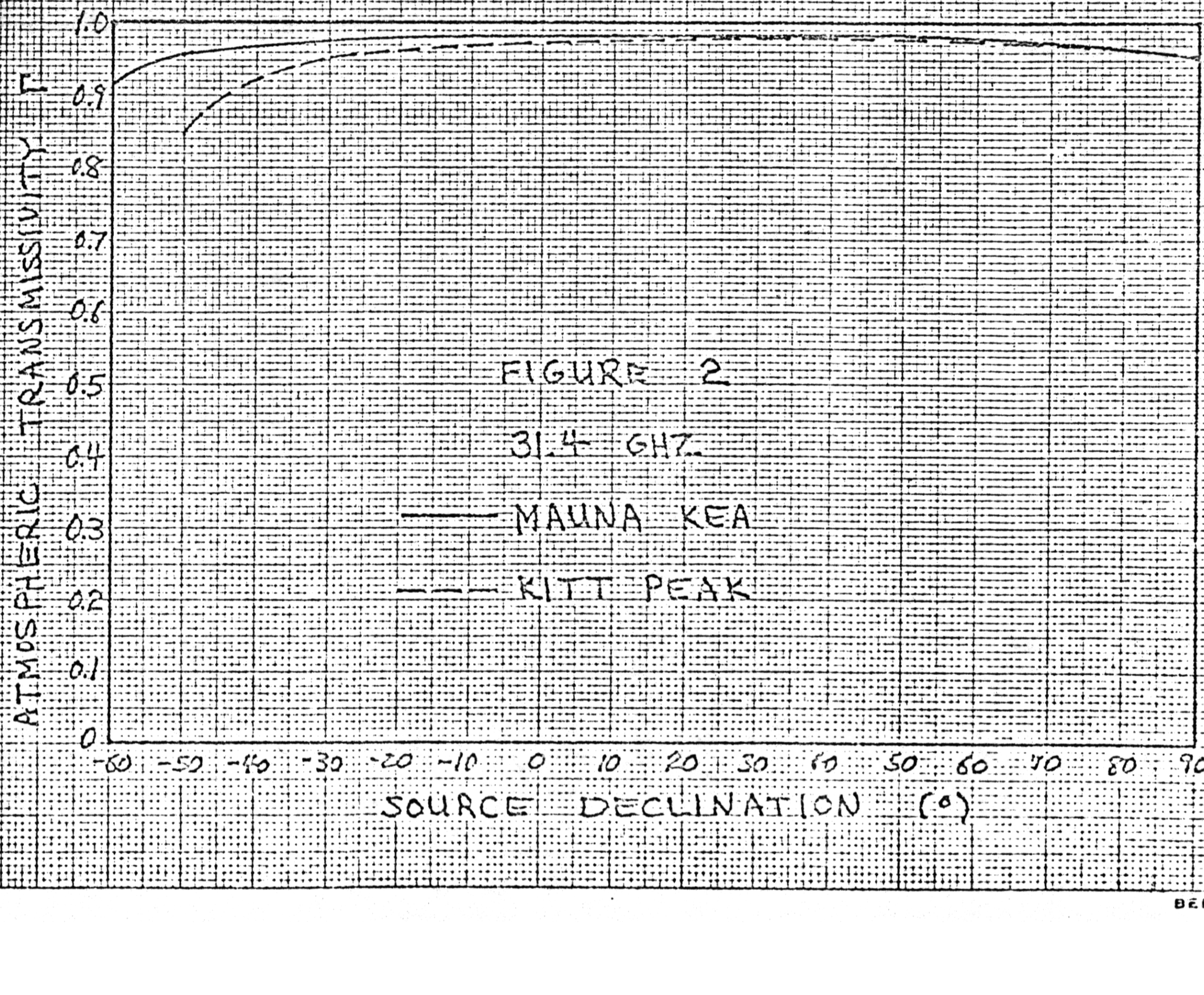
FIGURE 2
31.4 GHZ
MAUNA KEA
KITT PEAK
ATMOSPHERIC TRANSMISSIVITY Γ
1.0
0.9
0.8
0.7
0.6
0.5
0.4
0.3
0.2
0.1
0
-60 -50 -40 -30 -20 -10 0 10 20 30 40 50 60 70 80 90
SOURCE DECLINATION (°)

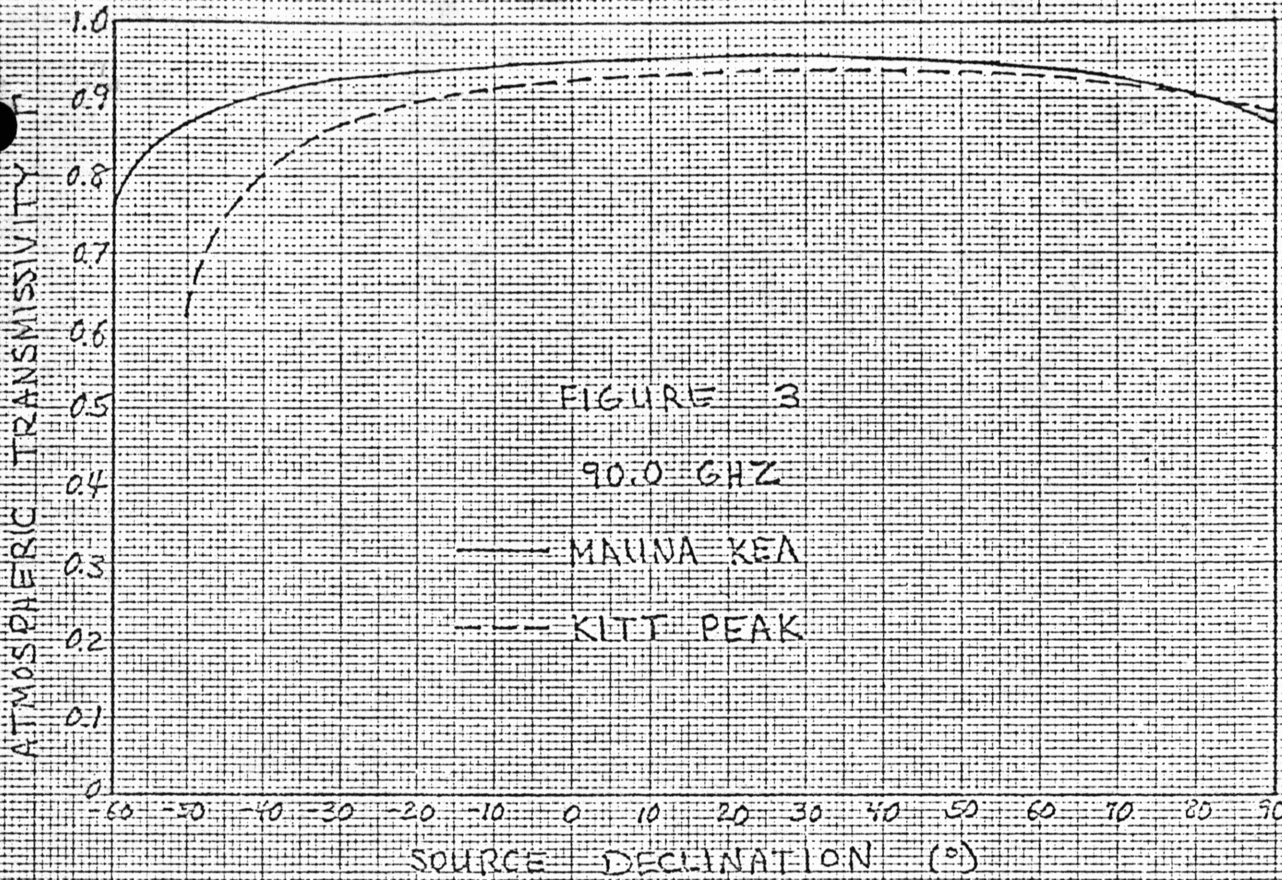
ATMOSPHERIC TRANSMISSIVITY η
1.0
0.9
0.8
0.7
0.6
0.5
0.4
0.3
0.2
0.1
0
FIGURE 3
90.0 GHZ
MAUNA KEA
KITT PEAK
-60 -50 -40 -30 -20 -10 0 10 20 30 40 50 60 70 80 90
SOURCE DECLINATION (°)

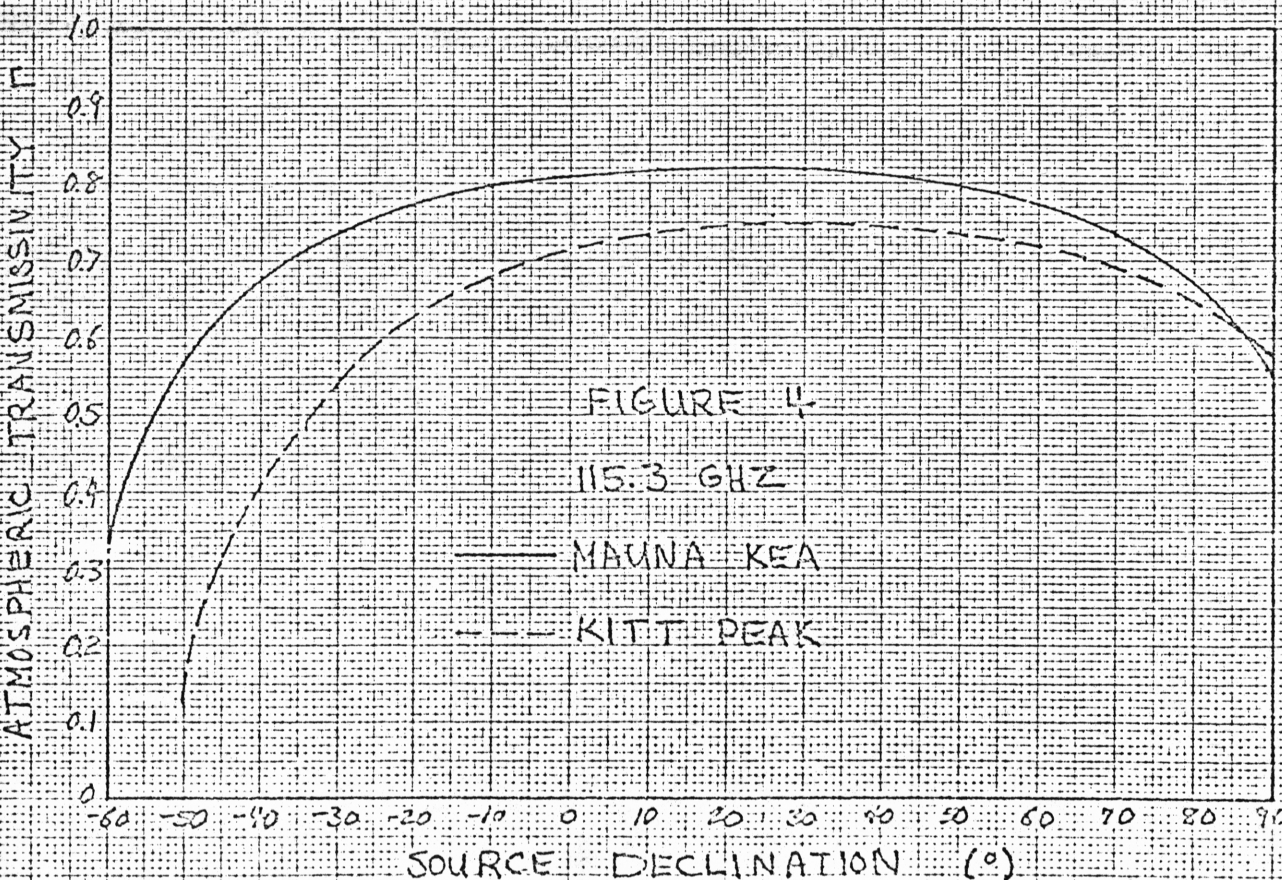
ATMOSPHERIC TRANSMISSIVITY η
1.0
0.9
0.8
0.7
0.6
0.5
0.4
0.3
0.2
0.1
0
FIGURE 4
115.3 GHZ
MAUNA KEA
KITT PEAK
-60 -50 -40 -30 -20 -10 0 10 20 30 40 50 60 70 80 90
SOURCE DECLINATION (°)

BEE M/M

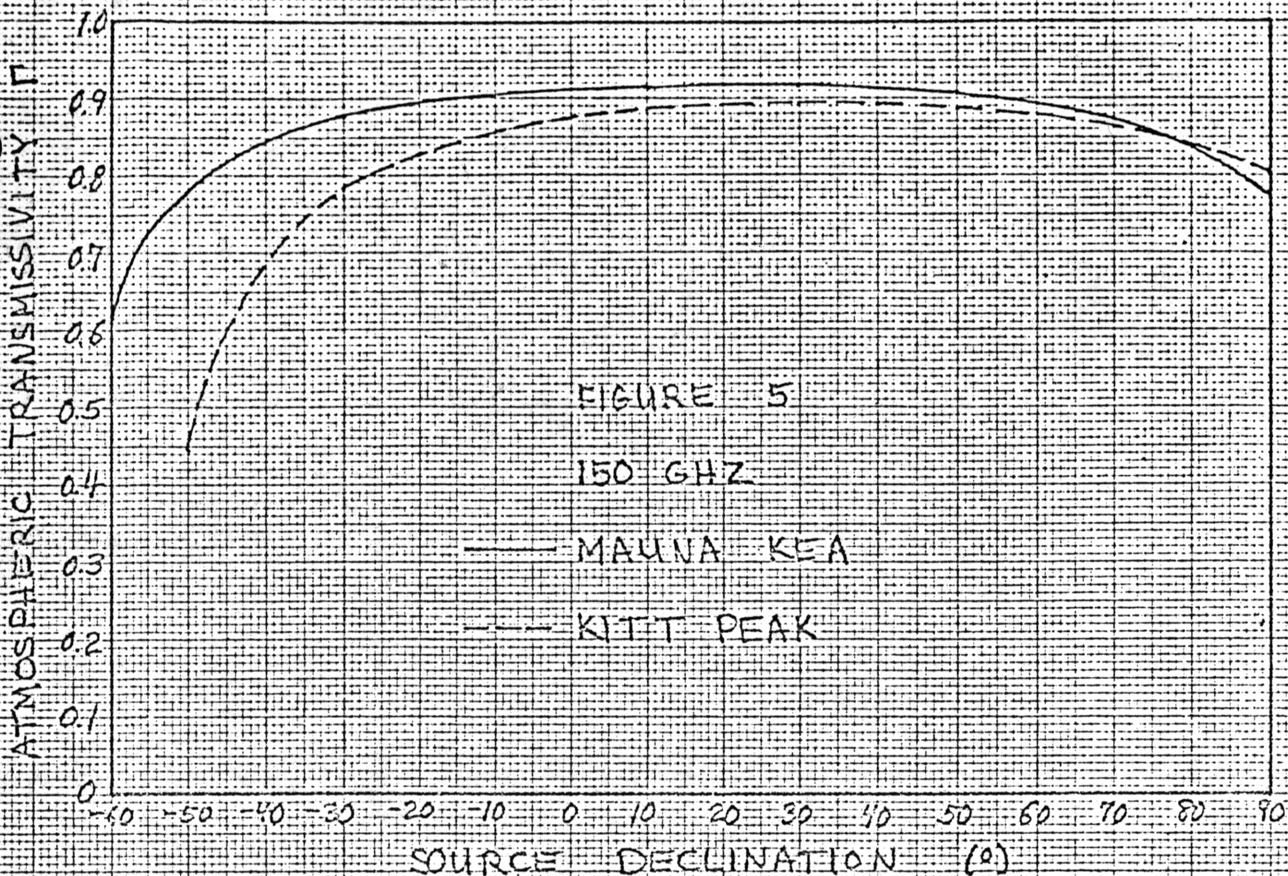
ATMOSPHERIC TRANSMISSIVITY Γ
1.0
0.9
0.8
0.7
0.6
0.5
0.4
0.3
0.2
0.1
0
-60 -50 -40 -30 -20 -10 0 10 20 30 40 50 60 70 80 90
SOURCE DECLINATION (°)
FIGURE 5
150 GHZ
MAUNA KEA
KITT PEAK

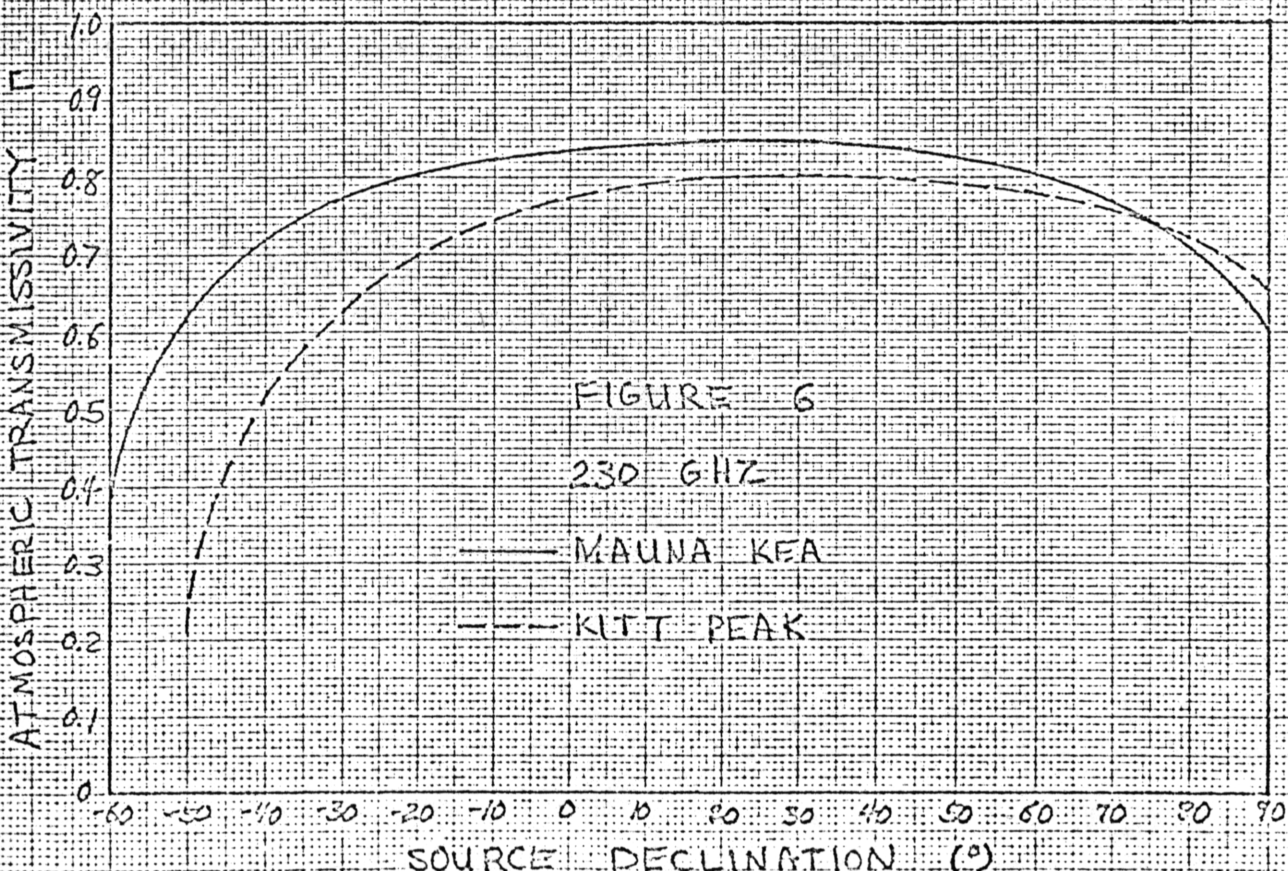
ATMOSPHERIC TRANSMISSIVITY Γ
1.0
0.9
0.8
0.7
0.6
0.5
0.4
0.3
0.2
0.1
0
-60 -50 -40 -30 -20 -10 0 10 20 30 40 50 60 70 80 90
SOURCE DECLINATION (°)
FIGURE 6
230 GHZ
MAUNA KEA
KITT PEAK

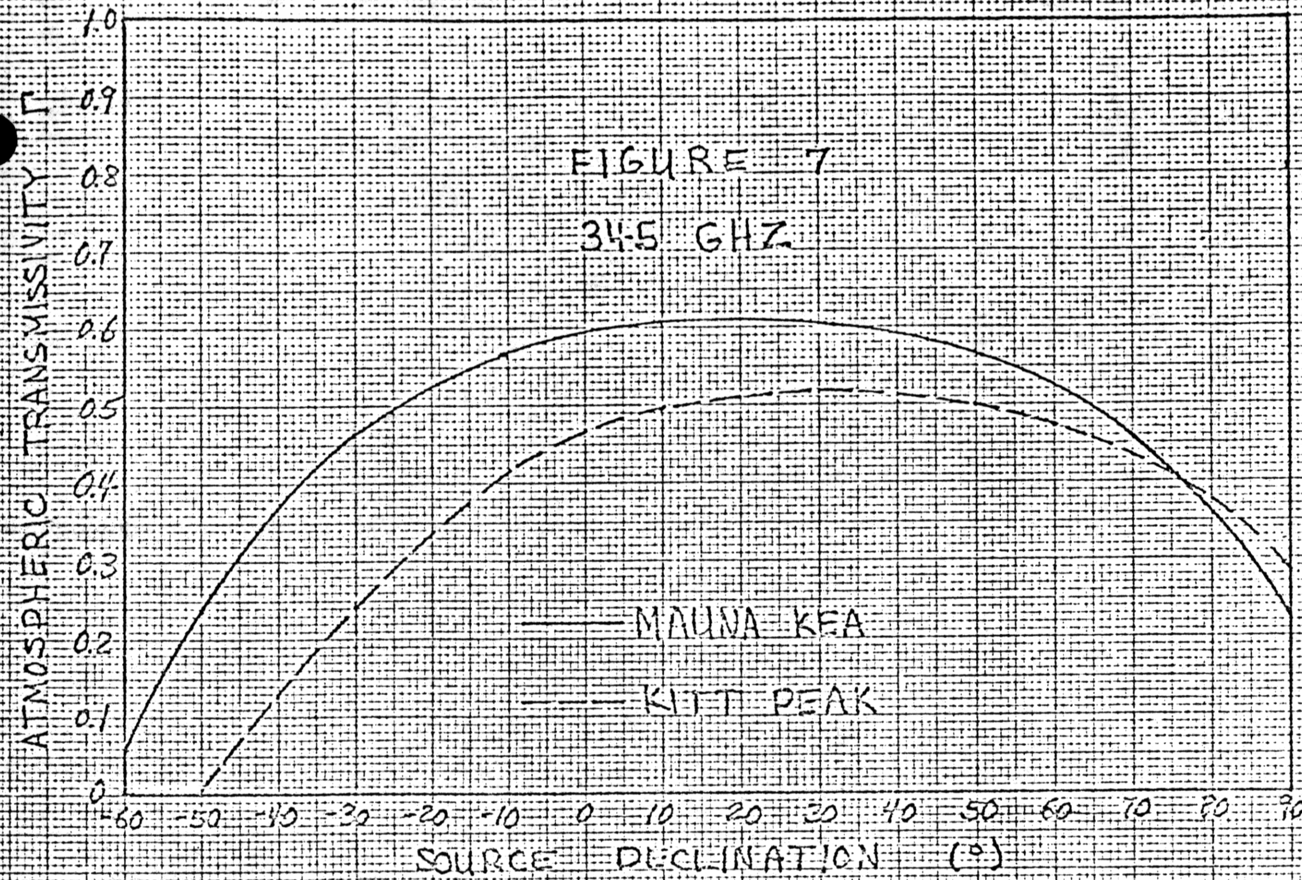
FIGURE 7
345 GHZ
ATMOSPHERIC TRANSMISSIVITY Γ
1.0
0.9
0.8
0.7
0.6
0.5
0.4
0.3
0.2
0.1
0
-60
-50
-40
-30
-20
-10
0
10
20
30
40
50
60
70
80
90
SOURCE DECLINATION (°)
MAUNA KEA
KITT PEAK

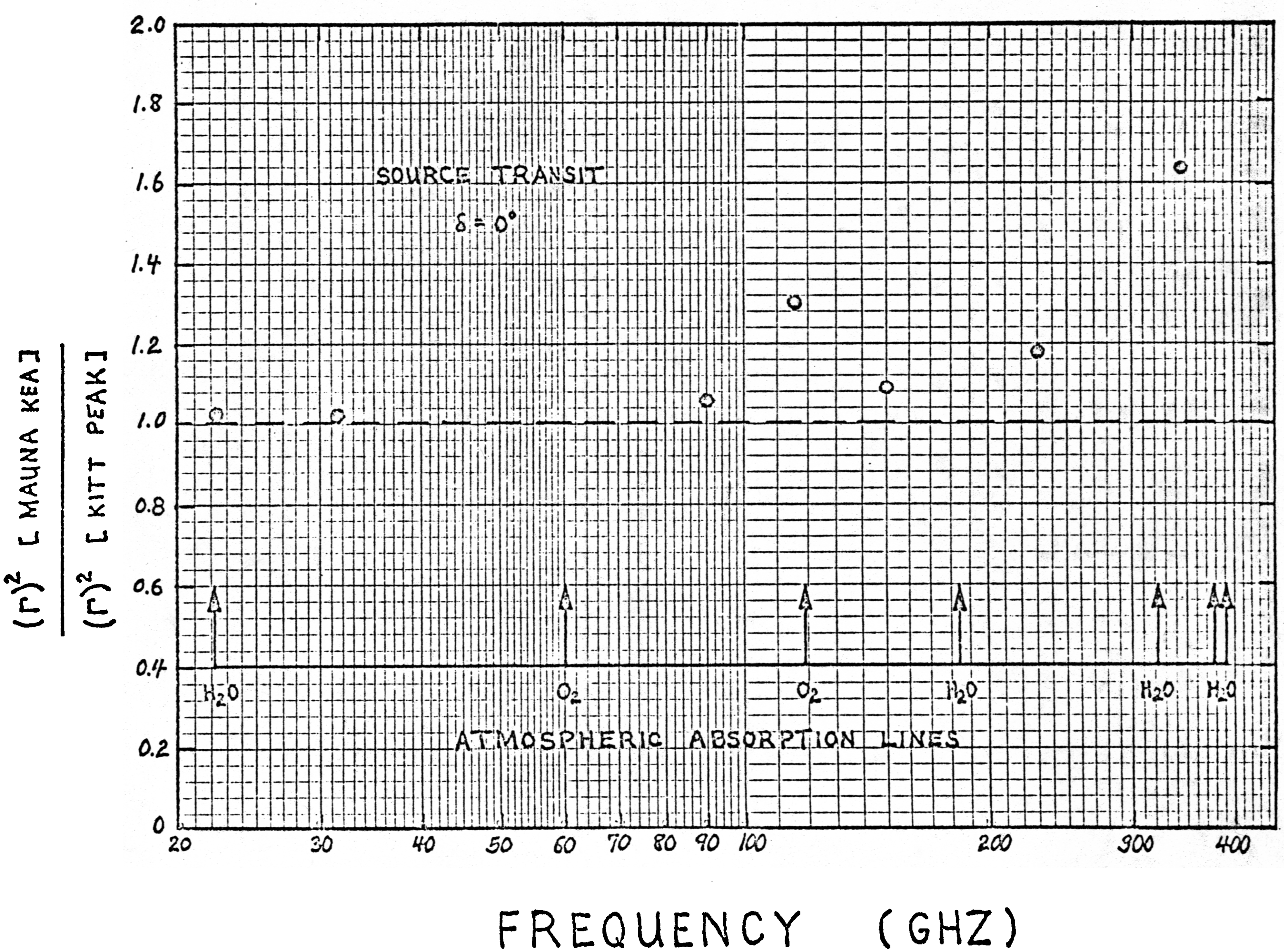

SOURCE TRANSIT
δ = 0°
$\frac{(\Gamma)^2 \text{ [MAUNA KEA]}}{(\Gamma)^2 \text{ [KITT PEAK]}}$
2.0
1.8
1.6
1.4
1.2
1.0
0.8
0.6
0.4
0.2
0
$H_2O$
$O_2$
$O_2$
$H_2O$
$H_2O$
$H_2O$
ATMOSPHERIC ABSORPTION LINES
20
30
40
50
60
70
80
90
100
200
300
400
FREQUENCY (GHZ)


FIGURE 8